J Mater Sci (2022) 57:21491–21501

Metals & corrosion

Effect of Co on the strengthening mechanisms of the creep-resistant 9% Cr-2%W-MoVNb steel

A. Fedoseeva[1,2,*], V. Dudko[1,2], N. Dudova[1], and R. Kaibyshev[2]

[1] Belgorod National Research University, Pobeda 85, Belgorod, Russian Federation 308015
[2] Russian State Agrarian University - Moscow Timiryazev Agricultural Academy, Timiryazevskaya, 49, Moscow, Russian Federation 127550

Received: 24 August 2022
Accepted: 4 November 2022
Published online: 15 November 2022

ABSTRACT

The alloying by 3 wt.% Co increases the tensile strength of the P92-type steel at elevated temperatures. The increments in the yield strength are 20%, 11% and 12% at testing temperatures of 500 °C, 600 °C and 650 °C, respectively, as compared with the Co-free P92-type steel. Cobalt strongly affects the strengthening due to the martensitic laths and dislocations regarding the lath growth and dislocation motion. The increases in the strengthening due the martensitic laths and the dislocations comprise 22, 43, 33 and 31 MPa at 20 °C, 500 °C, 600 °C and 650 °C, respectively. Reduction in initially higher dislocation density in the Co-containing steel occurs significantly less than that of the P92 steel at tensile tests at elevated temperatures. On the other hand, the influence of Co on interaction of free lattice dislocations with secondary particles or solid solution is negligible at tensile tests. The increments in the strengthening due to particles and solid solution are about 9% and 5%, respectively, at all tensile tests.

Introduction

Creep-resistant high-Cr martensitic steels are prospective materials for production of the pipes, tubes, steam lines and others elements for fossil-fuel power stations operating at temperatures up to 600–620 °C and pressure up to 25–30 MPa [1, 2]. The improved creep properties of these steels are contributed by the strengthening due to the martensitic laths, solid solution, particles and dislocations [3–6]. The addition of cobalt, tungsten, molybdenum, rhenium, copper, boron and others increases the creep resistance of 9–12% Cr steels because of retarding the dislocation rearrangement, knitting reactions between dislocations and lath boundaries, particle coarsening and other diffusion-controlled reactions [2, 4–12]. It is known that cobalt positively affects the creep resistance [2–4, 7–13]; the addition of 3 wt.% Co to the P911 and P92 steels leads to the 26% and 18% increase in the 100,000 h creep rupture strength at 650 °C,

Handling Editor: P. Nash.

Address correspondence to E-mail: fedoseeva@bsu.edu.ru
E-mail Addresses: dudko@bsu.edu.ru; dudova@bsu.edu.ru; rustam_kaibyshev@bsu.edu.ru

https://doi.org/10.1007/s10853-022-07940-z

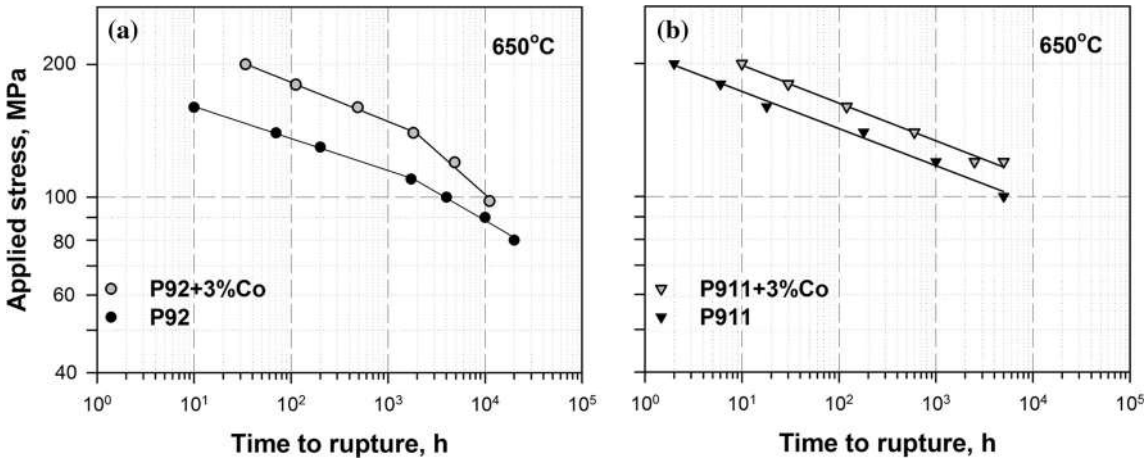

Figure 1 Creep properties of the Co-containing and Co-free **a** P92 [12] and **b** P911 [11] steels.

respectively, estimated using Larson-Miller parameter [11–13]. The effect of Co on creep properties of the P92 and P911 steels is represented in Fig. 1.

The reasons for the positive effect of cobalt on the creep properties have not yet been clarified, while some explanations have been proposed [2–4, 7–13]. First, cobalt was supposed to enhance the solid solution strengthening of steels [2, 3, 10]. However, this suggestion contradicts the results of studies [14–16] because the values of shear modulus and lattice parameter of Co and Fe atoms are close. Second, cobalt elevates the Curie temperature that leads to retarding the diffusion-controlled processes [9]. Third, cobalt provides the higher volume fraction of secondary phase particles [7] and slows down their coarsening [8, 9, 11, 12, 17, 18], although cobalt was found to increase the interfacial energy between precipitates and matrix [19]. So, the final mean size of $M_{23}C_6$ carbides decreases with 12–15% with addition of 3 wt.% Co to P911 and P92 steel after 30,000 h of aging at 650 °C [11, 12] and with 30% with addition of 10 wt.% Co to P92 after 30,000 h of aging at 600 °C [9]. The slowing down of particle coarsening is recognized as the main reason for increasing the stability of tempered martensite lath structure during creep and thermal exposure [9]. Fourth, cobalt suppresses the formation of δ-ferrite during austenitizing, which eliminates the local precipitation of MX carbonitrides within the δ-ferrite grains [2–10, 14, 16–18]. So, these facts evidence for the indirect influence of Co on the evolution of the structural parameters during creep or thermal exposure.

In the present research, we compare the Co-free and Co-containing P92-type steels. The creep properties of these steels were published previously [12, 13, 17–21]. The addition of 3 wt.% Co to P92-type steel enhanced the 100,000 h creep rupture strength from 72 [1] to 86 MPa [12]. However, the role of Co in increasing the creep strength of the Co-containing P92-type steel remains an open question. Therefore, the aim of this study is to compare behavior of the Co-free and 3% Co-containing P92-type steels under tensile tests at different temperatures and to evaluate the effect of Co addition on different strengthening mechanisms.

Materials and methods

The Co-free and Co-containing 9% Cr steels denoted here as the P92 and P92 + 3%Co steels, respectively, were obtained using air-induction melting at CNIITMASH Company, Moscow, Russia. The chemical compositions (in wt.%) of the steels studied are listed in Table 1.

The main difference of these steels is the Co content. Also these steels differ slightly in the content of Si, Mn and Ni. The samples for structural characterization and mechanical properties were machined from the hot-rolled rods with cross section of 15 mm × 15 mm which finally were normalized at 1050 °C for 30 min, air cooled and tempered at 750 °C for 3 h, air cooled. Tensile tests were performed on the flat samples with a length of 35 mm and cross section of 7 mm × 3 mm at a strain rate of 2×10^{-3} s^{-1} and temperatures of 20, 500, 600 and 650 °C up to failure using the «Instron 5882» testing machine.

Table 1 Chemical compositions of the Co-free and Co-containing steels (in wt.%)

Steel	C	Si	Mn	Cr	Ni	Mo	W	Co	Nb	V	N	B	Al	Fe
P92	0.10	0.17	0.54	8.75	0.21	0.51	1.6	–	0.07	0.23	0.04	0.003	0.013	Bal
P92 + 3%Co	0.12	0.08	0.23	9.46	0.04	0.44	2.0	3.1	0.06	0.21	0.05	0.005	0.009	Bal

A Jeol JEM-2100 transmission electron microscope (TEM) was used for examination of microstructure. Disks with a 3 mm diameter were cut from gage portions of ruptured tensile specimens and electropolished to perforation with a Tenupol-5 twinjet polishing unit using a 10% solution of perchloric acid in glacial acetic acid. The width of martensitic laths and particle size were measured on at least five selected TEM images. The dislocation observation was carried out under multiple-beam conditions with large excitation vectors for several diffracted planes for each TEM image. Differential scanning calorimetry (DSC) was performed on a ~ 60 mg specimens during heating to 1100 °C at a rate of 20 °C min^{-1} by using an SDT Q600 (TA Instruments) calorimeter. Modeling of the phase composition was carried out using Thermo-Calc software (TCFE7 database). The other details of the investigation of the mechanical properties and microstructure were presented in previous works [5, 11–13, 17–21].

Experimental results and discussion

Differential scanning calorimetry

Figure 2 demonstrates the DSC curves obtained under heating conditions of the Co-free and Co-containing P92 steels normalized at 1050 °C. It was found that the A_1 and A_3 temperatures were approximately 840 °C and 900 °C, respectively, for both steels. On the other hand, the addition of Co shifted the endothermic peak corresponding to the Curie temperature from 720 °C for the P92 steel to a higher temperature of 760 °C for the Co-containing steel. It should be noted that the Curie temperature of the P92 + 3Co steel is close to the tempering temperature.

Initial microstructure

The tempered microstructure of the steels studied was described in previous works in detail

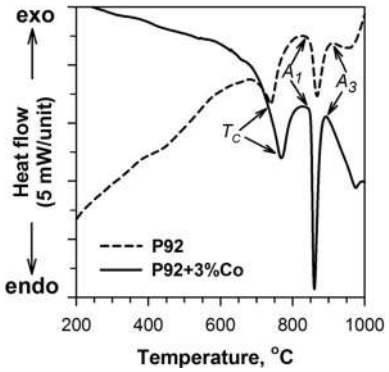

Figure 2 DSC curves obtained during heating of the Co-free and Co-containing P92 steels.

[12, 13, 17–21]. The formation of tempered martensitic lath structure with high dislocation density inside martensitic laths was observed under heat treatment consisting of normalizing and tempering in both steels (Fig. 3, Table 2).

The boundary Cr-rich $M_{23}C_6$ carbides with a mean size of 85–90 nm were dominant secondary phase in both steels (Fig. 3a). Nb-rich and V-rich MX carbonitrides with a mean size of 30 nm were randomly distributed in the ferritic matrix (Fig. 3b). No evidence for δ-ferrite appearance was revealed in both steels. The 3 wt.% Co addition led to the following changes in the tempered structure of the modified P92 steel as compared with Co-free P92 steel (Table 2):

- Twice decrease in the mean size of the prior austenite grains;
- Slight decrease in the lath width;
- 1.5 times increase in the dislocation density.

Mechanical properties

The engineering stress–strain curves at test temperatures of 20, 500, 600 and 650 °C are presented in Fig. 4a and b. The shape of curves was similar for both steels studied. When testing temperature increased, strength decreased and elongation-to-

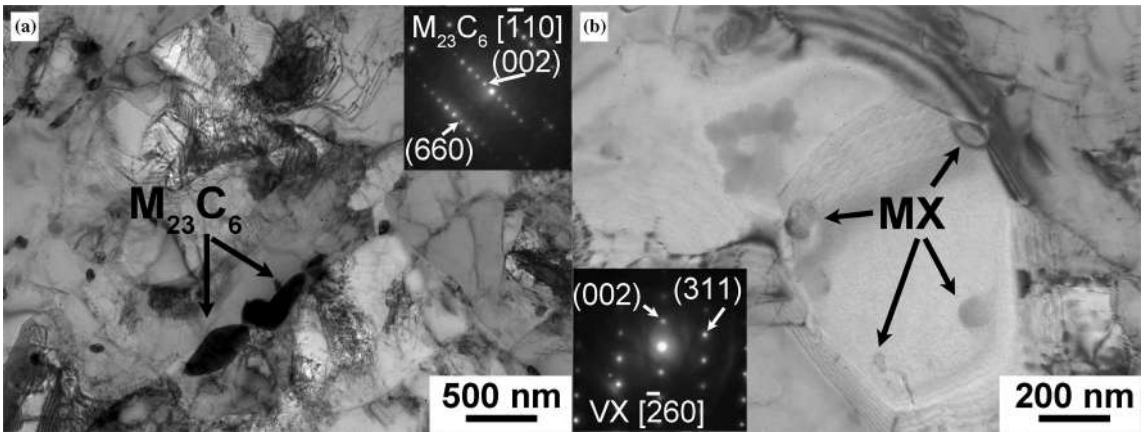

Figure 3 TEM image of the tempered martensite lath structure of the 9% Cr steel together with $M_{23}C_6$ carbides and MX carbonitrides and their corresponding selected area electron diffractions.

rupture increased (Fig. 4a and b). It can be seen that the Co-containing P92 steel exhibited higher stress than steel without Co (Fig. 4a and b). Figure 4c and d shows the difference between the yield strength (YS) and ultimate tensile strength (UTS) of two steels. At ambient temperature, the strength properties of both steels were close to each other. At 500 °C, the YS and UTS of Co-containing steel exceeded those of the P92 steel by approximately 20%. At 600 and 650 °C, an increase in the YS and UTS was about 11–12%. Thus, the alloying with 3 wt.% Co increases the tensile strength of the P92-type steel only at elevated temperatures.

Microstructures after tensile test

TEM images of the microstructures of the P92 and P92 + 3%Co steels after tensile tests at various temperatures are presented in Fig. 5. The structural parameters are summarized in Table 2. Note that the microstructural parameters after heat treatment and after tensile test at 20 °C were the same. This is common feature for both steels (Fig. 5, Table 2). In both steels, the lath widening and decrease in the dislocation density occurred during deformation with increasing the test temperature (Fig. 6a and b). At the same time, the sizes and volume fractions of the secondary phase particles and the amount of solutes in the ferritic matrix remained the same as in the tempered state (Fig. 5, Table 2). It seems that the addition of Co inhibited both the lath growth and drop in the dislocation density (Fig. 6a and b). Thus, after the 650 °C tensile test, an increase in the lath width by 45% and a decrease in the dislocation density by a factor of 2.5 in the P92 + 3%Co steel was less than the same change in the Co-free steel (67% and 4 times, respectively) (Fig. 6a and b, Table 2).

It is interesting to note that a strong linear correlation between the lath width (l) and the distance between dislocations determined as $\rho^{-0.5}$ was found for both steels (Fig. 6c) and can be written as follows:

$$l = 4.62\rho^{-0.5} \quad (1)$$

This indicates that Co addition does not change the relationship between the lath width and dislocations regardless of the test temperature.

Types of strengthening

The following strengthening mechanisms that contribute to the YS and UTS of the P92 and P92 + 3%Co steels were evaluated according to a model [3–5]:

(1) Lattice strengthening, which was estimated as $2 \times z\ 10^{-4} \times G$, where G is the temperature-dependent shear modulus. At 20 °C G = 84 GPa, at 500 °C G = 64 GPa, at 600 °C G = 60 GPa, at 650 °C G = 60 GPa.

(2) Solid solution strengthening (σ_{ss}) resulted from Cr, W, Mo, Ni, Mn, Si and Co atoms in the ferritic matrix was evaluated using Fleisher and Labusch as well as Nabarro theory [15] as follows [22]:

$$\sigma_{ss} = 1.1 \times 10^{-3} \frac{M\alpha^{4/3}\omega^{1/3}G}{b^{1/3}} \sum \varepsilon_{bi}^{4/3} c_i^{2/3} \quad (2)$$

where M is the Taylor factor for ferrite (2.54), α is set to the value of 4 for screw dislocations [23], ω is the range of the maximum interaction

Table 2 Structural parameters of both steels after tempering (initial state) and tensile tests

Structural parameters		P92 steel					P92 + 3%Co steel				
		Initial state	Tensile tests				Initial state	Tensile tests			
			20 °C	500 °C	600 °C	650 °C		20 °C	500 °C	600 °C	650 °C
PAG size, (μm)		20					10				
Lath width,(nm)		420	420	410	554	705	380	380	350	470	553
Dislocation density, × 10^{14} m^{-2}		1.7	1.7	1.00	0.6	0.4	2.0	2.0	2.0	1.3	0.8
$M_{23}C_6$/MX size, nm		85/30					90/30				
$M_{23}C_6$/MX volume fraction*, %		1.86/ 0.34	1.86/ 0.34	1.90/ 0.34	1.92/ 0.34	1.930.34/	2.29/ 0.34	2.29/ 0.34	2.30/ 0.34	2.33/ 0.34/	2.35/ 0.34
Content in matrix, wt.%/at.%	Co	0/0					3.0/3.0				
	Cr	7.50/8.15					8.50/9.23				
	W+Mo	1.64/0.63					1.97/0.71				
	Ni+Si+Mn	0.92/1.07					0.35/0.39				

*Estimated by thermo-calc software

force between a solute atom and dislocation and set to $5b$, b is the Burgers vector (2.48×10^{-10} m), ε_b is the size misfit parameters, c is the atomic fraction of the solute. The values of ε_b for different solute atoms used in the calculation were taken from Refs. [15, 24]. Content of elements in the ferritic matrix was estimated by EDX spectroscopy (Table 2) The short-term tensile deformation did not lead to Laves phase precipitation and, consequently, to any change in the chemical composition of the ferritic matrix (Table 2).

(3) Dislocation strengthening (σ_{disl}) was proposed using Taylor theory as follows [3–5]:

$$\sigma_{disl} = \alpha G b \sqrt{\rho} \tag{3}$$

where α is an iron polycrystalline constant (0.38), ρ is the total dislocation density (m^{-2}).

(4) Particle strengthening due to $M_{23}C_6$ carbides and MX carbonitrides after 20 °C, 500 °C and 600 °C tensile tests was estimated according to Orowan model as follows [5]:

$$\sigma_{Orowan} = 0.84 G b \Big/ \left(d\sqrt{\tfrac{\pi}{6f}} - d \right) \tag{4}$$

where f and d are the volume fraction and mean size of particles, respectively. We suggest the linear sum of contributions from $M_{23}C_6$ and MX particles. At 650 °C tensile test, particle strengthening was determined as the stress required to detach the dislocation from the particle after finishing the climb as follows [20, 25–27]:

$$\sigma_{detach} = G b \sqrt{1-k^2} \Big/ \left(d\sqrt{\frac{\pi}{6f}} \right) \tag{5}$$

where k is the relaxation parameter and is 0.85 [28]. Total σ_{detach} is suggested to be as $\sqrt{\sigma_{detach}(M_{23}C_6)^2 + \sigma_{detach}(MX)^2}$.

(5) Lath strengthening (σ_{lath}) was evaluated using Langford-Kohen model as follows [5]:

$$\sigma_{lath} = k_y (2l)^{-1} \tag{6}$$

where l is the mean transverse size of the martensitic laths/subgrains (μm), and k_y is a constant (86.2 MPa μm^{-2}) [5, 29].

A linear summation of these contributions gave the best coincidence between the experimental YS at 20 °C and UTS at elevated temperatures and the calculated values with errors less than 10% for both steels (Fig. 7, Table 3). The comparison of calculated contributions and experimental YS/UTS is presented in Fig. 7 and Table 3. The biggest contribution to YS/UTS of both steels at 20 °C, 500 °C and 600 °C was made by the solid solution and particle strengthening. It should be noted that the values of the solid solution and particle strengthening are close to each other. At 650 °C, particle strengthening decreased to the level of dislocation strengthening (Fig. 7b and d, Table 3). When the temperature of tensile test increased from 20 to 650 °C, the decrease in the contributions due to the martensitic laths and dislocations comprised 40% and 64%, respectively, for the P92 steel and 31% and 54%, respectively, for the

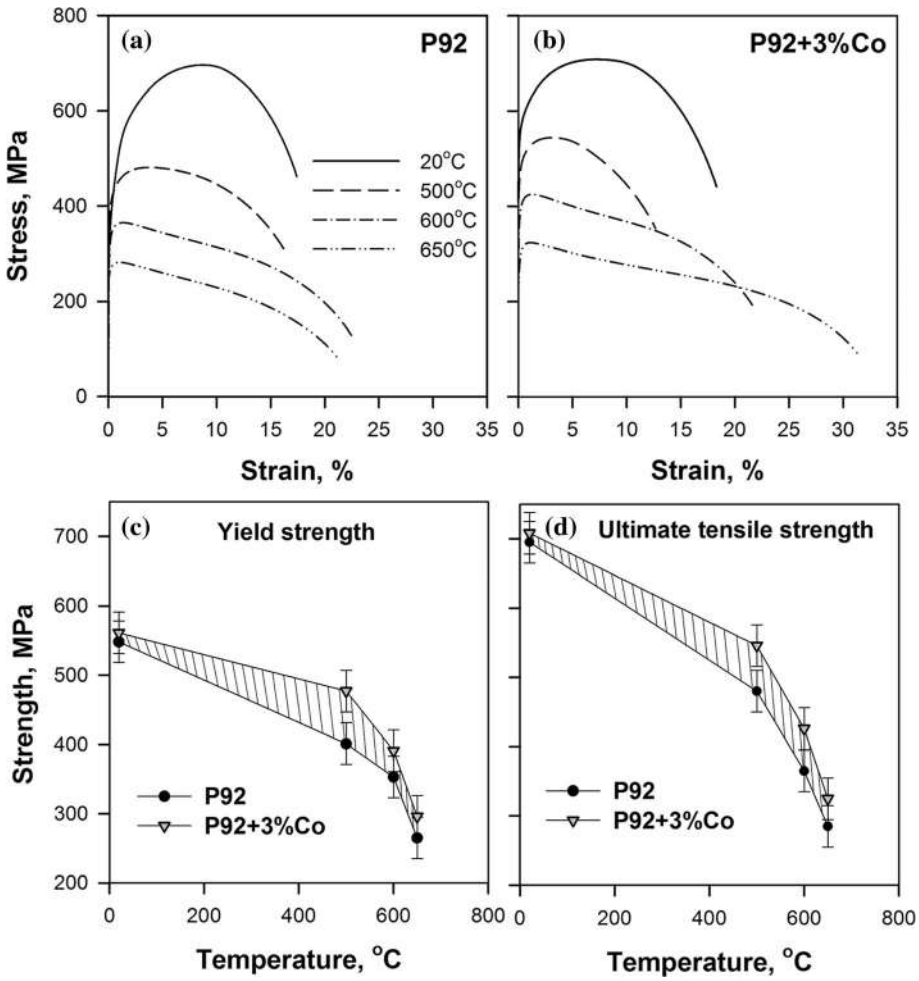

Figure 4 Engineering stress–strain curves for the P92 (**a**) and P92 + 3%Co (**b**) steels; the increase in the YS (**c**) and the UTS (**d**) of the Co-containing steel at different temperatures.

P92 + 3%Co steel. Such strong decrease in the dislocation and lath strengthening indicates the high mobility of dislocations and lath boundaries under stress condition [4]. As under creep conditions, tensile test at elevated temperatures leads to the lath growth due to the excess free dislocations within the martensitic laths [4]. So, the lath strengthening effect is created by the elimination of dislocation motion, and the lath growth decreases the retarding effect on the dislocation motion [30] as shown in Figs. 6 and 7. The Zener pinning pressures from the secondary phase particles are not high enough to prevent the lath growth during tension at elevated temperatures. The high dislocation density is considered to be the main source of back-stresses under creep. The addition of Co slows down the recovery of dislocation structure at elevated temperature (Fig. 6b). This might be attributed to the Co-induced sluggish diffusion kinetics in the matrix.

Effect of Co on strengthening contributions

The effect of Co on different strengthening mechanisms in the P92-type steel is presented in Fig. 8. The biggest increment in the strengthening contribution gives strengthening due to the martensitic laths and dislocations (Fig. 7b and d, Table 3), wherein the relationship between the lath width and dislocation density remains the same for both steels (Fig. 6c). It can be seen that the Co addition leads to the most increase in the strengthening due to the martensitic laths and dislocations as compared with Co-free P92 steel, whereas the particle and solid solution strengthening change insignificantly (Fig. 7, Table 3). At 20 °C tensile test, an increase in the strengthening due to martensitic laths and dislocations comprises 10–11% for each contribution (Fig. 8a and b, Table 3). Opposite, when the test temperature increases, the increment in strengthening due to laths and

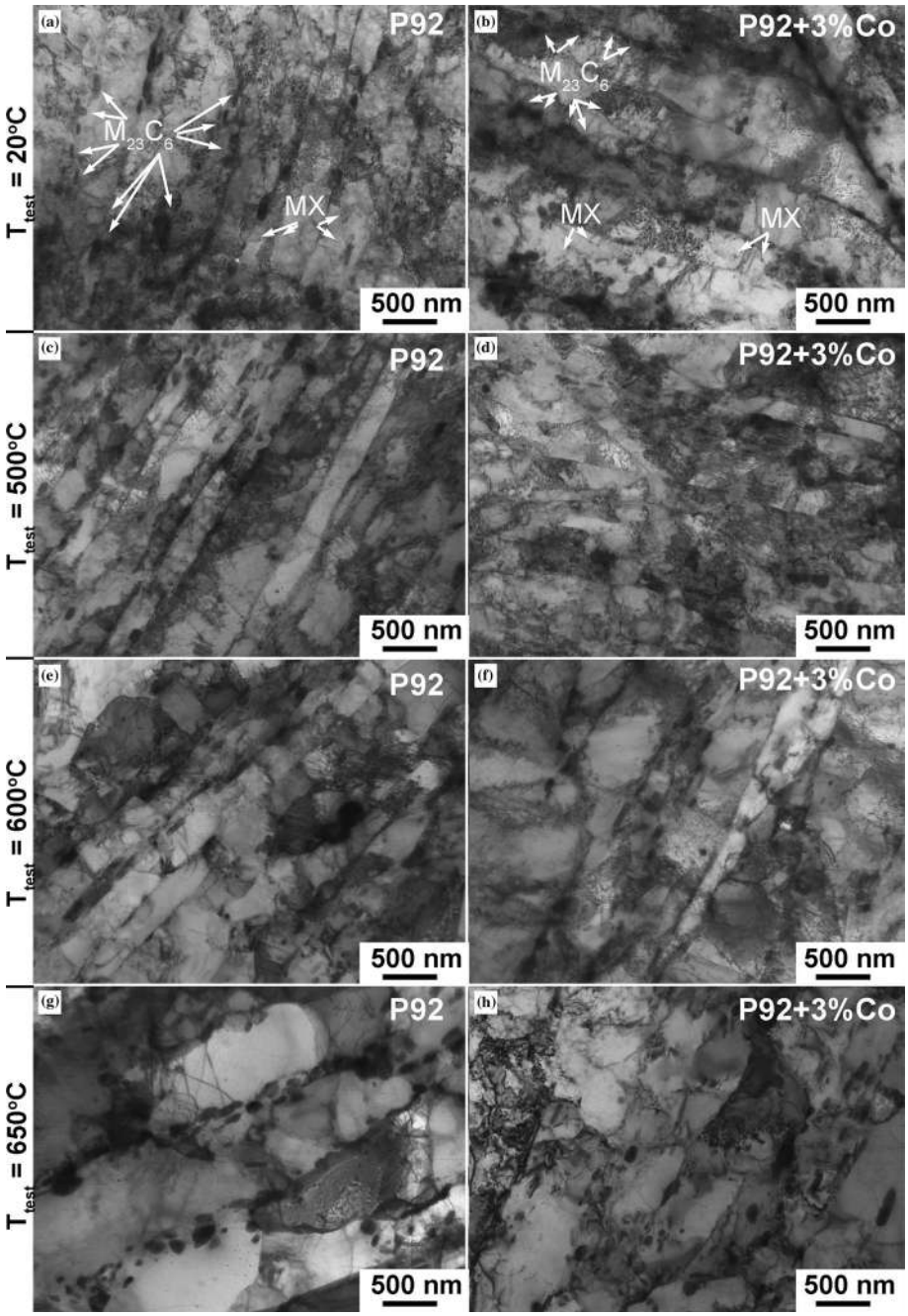

Figure 5 TEM images of the P92 (**a**–**d**) and P92 + 3%Co (**e**–**h**) steels after tensile tests at different temperatures.

dislocations increases significantly by 17–28% and 40–43%, respectively, as compared with P92 steel. This fact is attributed to the retaining the high dislocation density in the Co-containing steel in contrast to the P92 steel. So, the addition of Co slows down the recovery of dislocation structure at elevated temperatures (Fig. 6b). Higher dislocation density ensures the smaller lath width according to relationship in Fig. 6c. Tempering temperature of 750 °C is close to the Curie temperature of the P92 + 3%Co steel, which was 760 °C (Fig. 2), that provides the higher initial dislocation density in the tempered Co-containing steel (Table 2) due to the sluggish diffusion near and under the Curie temperature [9]. Nevertheless, cobalt does not tend to segregate in Fe matrix [31] and may have indirect effect on the retarding of dislocation motion through other elements. For example, Co decreases the tracer diffusion coefficient of Cr [9], which has solid solution strengthening [10] and interacts with mobile screw

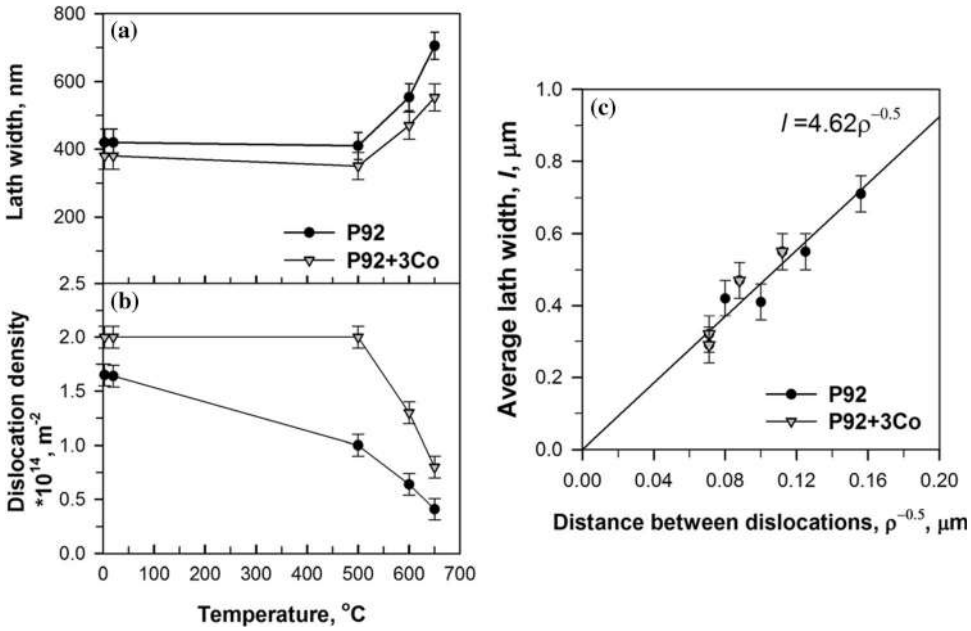

Figure 6 Change in the lath with **a** and dislocation density **b** of the P92 and P92 + 3%Co steels after tensile tests at different temperatures; **c** relationship between the lath width and distance between dislocations ($\rho^{-0.5}$) for both steels.

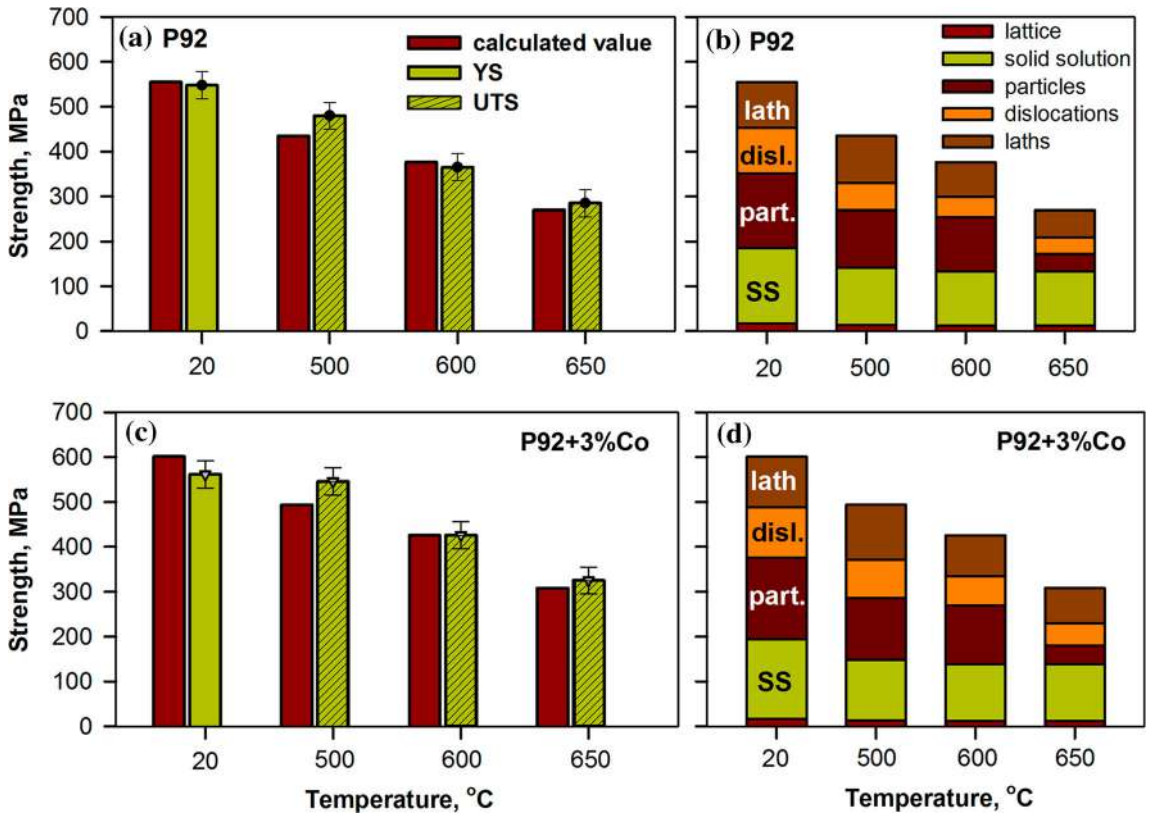

Figure 7 The comparison of the calculated and experimental values of the YS at 20 °C and UTS at elevated temperatures for the P92 (**a**, **b)** and P92 + 3%Co (**c**, **d)** steels.

dislocations that reduce their ability of slipping through matrix [2–4, 32]. In general, Co can have the similar effect on other elements.

An insignificant effect of Co on the particle strengthening is explained by the fact that cobalt is not included in the chemical compositions of

Table 3 Calculated strengthening contributions to the YS at 20 °C and UTS at elevated temperatures for the P92 and P92 + 3%Co steels

	P92				P92 + 3%Co			
Temperature of tensile test, °C	20	500	600	650	20	500	600	650
Lattice strengthening	16.8	12.8	12	12	16.8	12.8	12	12
Solid solution strengthening	169.4	129.0	121.0	121.0	177.6	135.3	126.8	126.8
Dislocation strengthening	101.4	60.3	45.2	36.2	111.9	85.3	64.5	50.6
Particle strengthening	165.7	128.0	120.8	39.4	181.2	138.1	130.4	40.7
Lath strengthening	102.4	105.1	77.8	61.1	113.4	123.1	91.7	77.9

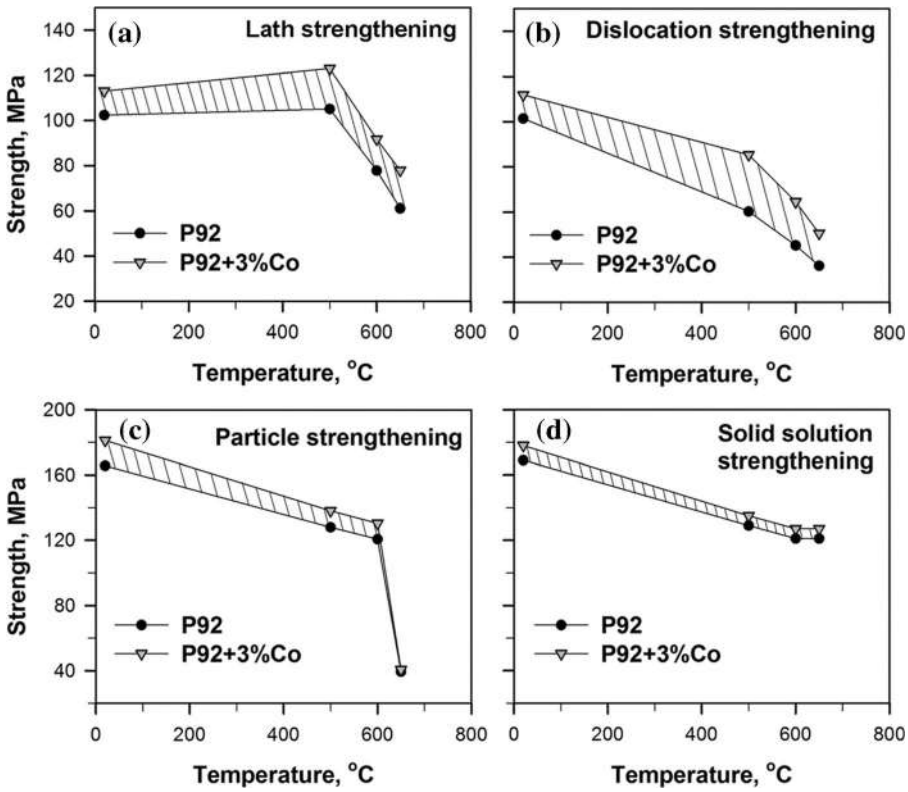

Figure 8 The increment in calculated strengthening due to laths (**a**), dislocations (**b**), particles (**c**) and solid solution (**d**) with 3 wt.% Co at different temperatures.

boundary $M_{23}C_6$ carbides and/or MX carbonitrides randomly distributed within ferritic matrix. In Ref. [7] mentioned that Co was found to increase the volume fraction of the secondary phase particles. The present results also confirm this suggestion (Table 2). The increase in the total volume fraction of $M_{23}C_6$ carbides and MX carbonitrides estimated by Thermo-Calc software due to addition of 3%Co comprises 18–20% (Table 2). However, higher fraction of precipitates leads to an increase in the particle strengthening of the P92 + 3%Co steel by only 8–9% at 20 °C, 500 °C and 600 °C (Fig. 8c and Table 3), when the interaction of dislocations with particles is described by the Orowan mechanism. This fact is in accordance with Ref. [9], in which the addition of 10 wt.% Co to the P92 steel gives rise to the Orowan stress with 30% at 600 °C. At higher temperature of 650 °C, the change in the particle strengthening mechanism was revealed. Detachment of dislocations from precipitates after finishing the climb [21, 25–27] at 650 °C was confirmed by the comparison of the calculated strengthening contributions and the experimental UTS. The increment in the particle strengthening at 650 °C in the P92 + 3%Co steel comprises only + 3% (Fig. 8c and Table 3). So, Co does not affect the interaction between the dislocations and precipitates.

It was expected that Co should contribute to the solid solution strengthening [2, 3, 10]. However, according to Fig. 8d and Table 3, the solid solution strengthening increases only by 5% due to 3 wt.% Co addition. This fact may be partially associated with the influence of

other elements in the steels studied. The sum contribution due to Σ(Si,Mn,Ni) contents (almost 1 wt.%) in the P92 steel compensates 3 wt.% Co in the P92 + 3%Co steel. In the Ref. [14–16], it was noticed that Co has a small size misfit with ferrite, which is an order of magnitude lower than that of Ni, Si or Mn. On the other hand, the ferritic matrix in the P92 + 3%Co steel is more enriched by Σ (Cr + W + Mo) solutes (Table 1) than in the P92 steel since the total content of these elements is approximately 1 wt.% higher in the Co-containing steel, which certainly provides an increase in the solid solution strengthening of this steel. So, the results obtained show that Co does not affect significantly the solid solution strengthening of P92-type steels. This is in accordance with Ref. [15, 16, 31] reported that Co does not change the elastic moduli of ferrite and does not produce the solid solution hardening or softening.

Conclusions

An increase in the yield strength and ultimate tensile strength due to addition of 3 wt.% Co in the P92-type steel at ambient and elevated temperatures has been revealed. It is shown that alloying by Co inhibits the widening of martensitic laths and provides retaining of higher dislocation density during tensile deformation that strongly increases the lath and dislocation strengthening as compared with the Co-free P92 steel. The addition of Co increases the Curie temperature to 760 °C that is close to tempering temperature, providing a higher initial dislocation density before tensile tests. Co slows down the recovery of dislocation structure at elevated temperatures. For both Co-free P92 and Co-containing steels, the dependence between the lath width and dislocation density obeys a relationship $l = 4.62\rho^{-0.5}$. The effect of Co on both solid solution strengthening and particle strengthening is insignificant.

Acknowledgements

The authors acknowledge with gratitude the financial support received through the Russian Science Foundation, under Grant No. 19-73-10089-П. The work was carried out using equipment of the Joint Research Center of Belgorod State National Research University «Technology and Materials» the activity of which was supported from the Ministry of Science and Higher Education of the Russian Federation within the framework of agreement No. 075-15-2021-690 (unique identifier for the project RF-2296.61321X0030). The authors are grateful to PhD-student I. Nikitin for sample preparation.

Declarations

Conflict of interest The authors declare that they have no conflict of interest.

References

[1] GianfrancescoDi A (2017) Materials for ultra-supercritical and advanced ultra-supercritical power plants. Woodhead Publishing, Cambridge

[2] Abe F, Kern T-U, Viswanathan R (2008) Creep-resistant steels. Woodhead Publishing, Cambridge

[3] Maruyama K, Sawada K, Koike J (2001) Strengthening mechanisms of creep resistant tempered martensitic steel. ISIJ Int 41:641–653. https://doi.org/10.2355/isijinternational.41.641

[4] Abe F (2008) Precipitate design for creep strengthening of a 9%Cr tempered martensitic steel for ultra-supercritical power plants. Sci Techn Adv Mater 9:013002. https://doi.org/10.1088/1468-6996/9/1/013002

[5] Nikitin I, Fedoseeva A, Kaibyshev R (2020) Strengthening mechanisms of creep-resistant 12%Cr–3%Co steel with low N and high B contents. J Mater Sci 55:7530–7545. https://doi.org/10.1007/s10853-020-04508-7

[6] Fedoseeva A, Nikitin I, Dudova N, Kaibyshev R (2019) On effect of rhenium on mechanical properties of a high-Cr creep resistant steel. Mater Lett 269:81–84. https://doi.org/10.1016/j.matlet.2018.10.081

[7] Helis L, Toda Y, Hara T, Miyazaki H, Abe F (2009) Effect of cobalt on the microstructure of tempered martensitic 9Cr steel for ultra-supercritical power plants. Mater Sci Eng A 510–511:88–94. https://doi.org/10.1016/j.msea.2008.04.131

[8] Yamada K, Igarashi M, Muneki S, Abe F (2003) Effect of Co addition on microstructure in high Cr ferritic steels. ISIJ Int 43:1438–1443. https://doi.org/10.2355/isijinternational.43.1438

[9] Gustafson Å, Ågren J (2001) Possible effect of Co on coarsening of M23C6 carbide and orowan stress in a 9% Cr steel. ISIJ Int 41:356–360. https://doi.org/10.2355/isijinternational.41.356

[10] Klueh RL (2005) Elevated temperature ferritic and martensitic steels and their application to future nuclear reactors. Int Mater Rev 50:287–310. https://doi.org/10.1179/174328005X41140

[11] Kipelova A, Odnobokova M, Belyakov A, Kaibyshev R (2013) Effect of Co on creep behavior of a P911 steel. Metall Mater Trans A 44:577–583. https://doi.org/10.1007/s11661-012-1390-3

[12] Dudova N, Plotnikova A, Molodov D, Belyakov A, Kaibyshev R (2012) Structural changes of tempered martensitic 9%Cr-2%W-3%Co steel during creep at 650°C. Mater Sci Eng A 534:632–639. https://doi.org/10.1016/j.msea.2011.12.020

[13] Fedoseeva A, Dudova N, Kaibyshev R (2016) Creep strength breakdown and microstructure evolution in a 3%Co modified P92 steel. Mater Sci Eng A 654:1–12. https://doi.org/10.1016/j.msea.2015.12.027

[14] Barrett RA, O'Donoghue PE, Leen SB (2018) A physically-based high temperature yield strength model for 9Cr steels. Mater Sci Eng A 730:410–424. https://doi.org/10.1016/j.msea.2018.05.086

[15] Leslie WC (1972) Iron and its dilute substitutional solid solutions. Metall Trans 3:5–26. https://doi.org/10.1007/BF02680580

[16] Spitzig WA, Leslie WC (1971) Solid solution softening and thermally activated flow in alloys of Fe with 3 at.% Co Ni or Si. Acta Metall 19:1143–1152. https://doi.org/10.1016/0001-6160(71)90046-0

[17] Fedoseeva A, Nikitin I, Dudova N, Kaibyshev R (2018) Strain-induced z-phase formation in a 9% Cr-3% Co martensitic steel during creep at elevated temperature. Mater Sci Engin A 724:29–36. https://doi.org/10.1016/j.msea.2018.03.081

[18] Fedoseeva A, Dudova N, Kaibyshev R (2016) Effect of tungsten on a dispersion of M(C, N) carbonitrides in 9 % Cr steels under creep conditions. Trans Indian Inst Met 69:211–215. https://doi.org/10.1007/s12666-015-0767-6

[19] Fedoseeva A, Tkachev E, Dudko V, Dudova N, Kaibyshev R (2017) Effect of alloying on interfacial energy of precipitation/matrix in high-chromium martensitic steels. J Mater Sci 52:4197–4209. https://doi.org/10.1007/s10853-016-0654-5

[20] Dudko V, Belyakov A, Molodov D, Kaibyshev R (2013) Microstructure evolution and pinning of boundaries by precipitates in a 9 pct Cr heat resistant steel during creep. Metall Mater Trans A 44:S162–S172. https://doi.org/10.1007/s11661-011-0899-1

[21] Dudko V, Belyakov A, Kaibyshev R (2017) Evolution of lath substructure and internal stresses in a 9% Cr steel during creep. ISIJ Int 57:540–549. https://doi.org/10.2355/isijinternational.ISIJINT-2016-334

[22] Sieurin H, Zander J, Sandstrom R (2006) Modelling solid solution hardening in stainless steels. Mater Sci Eng A 415:66–71. https://doi.org/10.1016/j.msea.2005.09.031

[23] Walbruhl M, Linder D, Ågren J, Borgenstam A (2017) Modelling of solid solution strengthening in multicomponent alloys. Mater Sci Eng A 700:301–311. https://doi.org/10.1016/j.msea.2017.06.001

[24] Terada D, Yoshida F, Nakashima H, Abe H, Kadoya Y (2002) *In-situ* observation of dislocation motion and its mobility in Fe-Mo and Fe-W solid solutions at high temperatures. ISIJ Int 42:1546–1552. https://doi.org/10.2355/isijinternational.42.1546

[25] Spigarelli S, Cerri E, Bianchi P, Evangelista E (1999) Interpretation of creep behaviour of a 9Cr–Mo–Nb–V–N (T91) steel using threshold stress concept. Mater Sci Technol 15:1433–1440. https://doi.org/10.1179/026708399101505428

[26] Magnusson H, Sandström R (2007) The role of dislocation climb across particles at creep conditions in 9 to 12 pct Cr steels. Metall Mater Trans A 38:2428–2434. https://doi.org/10.1007/s11661-007-9280-9

[27] Eliasson J, Gustafson A, Sandström R (2000) Kinetic modelling of the influence of particles on creep strength. Key Eng Mater 171–174:277–284. https://doi.org/10.4028/www.scientific.net/KEM.171-174.277

[28] Rosler J, Arzt E (1990) A new model-based equation for dispersion strengthened materials. Acta Metall Mater 38:671–683. https://doi.org/10.1016/0956-7151(90)90223-4

[29] Langford G, Cohen M (1969) Strain hardening of iron by severe plastic deformation. ASM-Trans 62:623–638

[30] Mitsuhara M, Yamasaki Sh, Miake M, Nakashima H, Nishida M, Kusumoto J, Kanaya A (2016) Creep strengthening by lath boundaries in 9Cr ferritic heat-resistant steel. Phil Mag Lett 96:76–83. https://doi.org/10.1080/09500839.2016.1154200

[31] Medvedeva N, Murthy A, Richards V, Van Aken D, Medvedeva J (2013) First principle study of cobalt impurity in bcc Fe with Cu precipitates. J Mater Sci 48:1377–1386. https://doi.org/10.1007/s10853-012-6884-2

[32] Mao Ch, Liu Ch, Yu L, Li H, Liu Y (2018) Mechanical properties and tensile deformation behavior of a reduced activated ferritic-martensitic (RAFM) steel at elevated temperatures. Mater Sci Eng A 725:283–289. https://doi.org/10.1016/j.msea.2018.03.119